AGU
ADVANCING EARTH AND SPACE SCIENCE

Geophysical Research Letters®

Key Points:

- High fraction of melt-freeze forms causes significant higher snow densities in the northwestern than in the eastern Weddell Sea
- Lower thermal conductivity of snow in the eastern Weddell Sea than previously assumed results in significantly reduced potential bottom sea ice growth
- In the northwestern Weddell Sea, the substantial amount of snow ice leads to additional thermodynamic ice growth at the ice bottom

Sensitivity of Sea Ice Growth to Snow Properties in Opposing Regions of the Weddell Sea in Late Summer

Stefanie Arndt[1] [ID]

[1]Alfred-Wegener-Institut Helmholtz-Zentrum für Polar- und Meeresforschung, Bremerhaven, Germany

Abstract The sensitivity of sea ice to the contrasting seasonal and perennial snow properties in the southeastern and northwestern Weddell Sea is not yet considered in sea ice model and satellite remote sensing applications. However, the analysis of physical snowpack properties in late summer in recent years reveals a high fraction of melt-freeze forms resulting in significant higher snow densities in the northwestern than in the eastern Weddell Sea. The resulting lower thermal conductivity of the snowpack, which is only half of what has been previously assumed in models in the eastern Weddell Sea, reduces the sea ice bottom growth by 18 cm during winter. In the northwest, however, the potentially formed snow ice thickness of 22 cm at the snow/ice interface contributes to additional 7 cm of thermodynamic ice growth at the bottom. This sensitivity study emphasizes the enormous impact of unappreciated regional differences in snowpack properties on the thermodynamic ice growth.

Plain Language Summary The sea ice cover in the Weddell Sea shows different ice age classes and can therefore be considered as a representative basin of the ice-covered Southern Ocean: while seasonal sea ice is found in the eastern Weddell Sea, it tends to be perennial in the west. Due to the year-round Antarctic snow cover, this age classification also applies for the snow column. However, the associated regional differences in snow properties and snow-to-ice conversion processes at the snow/ice interface are not yet considered in both sea ice model and satellite remote sensing applications when retrieving, for example, sea ice thickness. Based on recent snow observations in the region, regionally adjusted values for snow density and thermal conductivity could be determined. While the adjusted parameters result in attenuated ice growth in the eastern Weddell Sea, significant snow ice formation causes additional thermodynamic ice growth in the western Weddell Sea.

1. Introduction

The Weddell Sea is the key region in the ice-covered Southern Ocean, as it contains the largest fraction of the perennial Antarctic sea ice (e.g., Lee et al., 2017; Parkinson & DiGirolamo, 2021). The variability of the seasonal pan-Antarctic sea ice minimum is therefore mainly driven by the summer sea ice extent in the Weddell Sea. Accordingly, the region accounted for 36% of the contribution to the strong sea ice decrease in the summer of 2016/17 the most of any region, highlighting the importance of the Weddell Sea for heat and momentum exchange processes between atmosphere, sea ice, ocean, and the biogeochemical system in the ice-covered Southern Ocean (e.g., Jena et al., 2022; Vernet et al., 2019). The presence of snow on the ice strongly alters these interactions through its impact on the ice mass balance and related heat fluxes. In particular for Antarctic sea ice, the role of snow is heightened as the ice remains snow-covered throughout the year in most regions (Massom et al., 2001) causing a widespread negative ice freeboard, with the refreezing seawater-soaked snow forming so-called snow ice (e.g., Eicken et al., 1994; Tian et al., 2020). In addition, the snow column experiences strong seasonal changes in density, conductivity, water content, microstructure, and stratification, modifying significantly the sea ice energy and mass budgets (e.g., Massom et al., 2001; Nicolaus et al., 2009).

As such, Arndt and Paul (2018) have shown that one of the main drivers of the variability in first-year and multi-year snow properties is the variability in snow stratigraphy, in particular the grain size distribution, which is closely linked to the prevailing seasonal snow metamorphism. The stages of snow metamorphism vary strongly on spatial scales as, on the one hand, the perennial snow cover is much more metamorphosed than the seasonal one (Nicolaus et al., 2009). On the other hand, the snowmelt onset dates derived from satellite remote sensing data show a latitudinal dependence, with an earlier melt onset in the marginal ice zone, and melt spreading southward as summer progresses (e.g., Arndt & Haas, 2019; Arndt et al., 2016). The resulting different snow grain type distributions in the vertical snow column modify the corresponding bulk densities with layer densities

ranging from less than 100 kg m^{-3} for new snow to 290 kg m^{-3} for depth hoar up to 760 kg m^{-3} for icy layers (Massom et al., 2001; Sturm et al., 1998). At the same time, the snow layer density determines its effective heat conductivity and therefore the ability of the snow to insulate the underlying Antarctic sea ice cover, governing the thermodynamic ice growth (Calonne et al., 2011; Sturm et al., 1997). Thus, for the eastern sector of the Southern Ocean and in the Bellingshausen, Amundsen, and Ross Seas, Fichefet et al. (2000) have shown that using values for the thermal conductivity of snow reduced by half from the literature (0.31 W m^{-1} K^{-1}, e.g., Hibler (1979)) significantly improves the ice thickness distribution in the region as thermodynamic ice growth is reduced by 10% on average.

This highlights the need to distinguish not only between annual and perennial sea ice but also to consider the corresponding snow cover differences. However, current implementations of snow properties in climate models as well as in satellite remote sensing data products usually use global parameterizations for snow properties. Based on that, the question arises how sensitive sea ice growth is to the described different seasonal snow properties in the opposing regions, that is, the seasonal and perennial ice regime. Therefore, to assess these regional variations, observed late-summer snow properties from ice stations sampled in recent years in the northwestern and southeastern Weddell Sea were analyzed. To put the observations into a broader temporal and spatial context, measurements from autonomous ice-tethered platforms were added. To quantify the actual sensitivities to ice thickness growth, the determined snow parameters were applied in a respective sensitivity study using a simple one-dimensional thermodynamic ice growth model.

2. Data and Methods

2.1. In Situ Data and Analysis

Field measurements used in this study were carried out during three expeditions of the German research icebreaker *RV Polarstern* to the Weddell Sea in late austral summer, that is, from January to March. While the ice station work during expedition PS118 covered the northwestern Weddell Sea in 2019 (Arndt & Haas, 2021; Haas et al., 2019), the ice stations of expeditions PS111 (Arndt et al., 2018), and PS124 (Haas et al., 2021) covered the southeastern Weddell Sea in 2018 and 2021, respectively (Figure 1). A total of 14 ice floes in the northwestern Weddell Sea and 21 ice floes in the pack ice of the southeastern Weddell Sea were visited by helicopter to study physical and biogeochemical properties of sea ice and snow. Here, snowpack analysis focused on the snow depth, snow density, and its stratigraphy.

Snow depth was measured along up to 1,200 m long transect lines with a horizontal resolution of 1–2 m across the entire floes with a GPS-equipped Magna Probe (Snow Hydro (Sturm & Holmgren, 2018)). The measurements were mostly accompanied by ground-based multifrequency electromagnetic induction measurements (GEM-2, Geophex Ltd., Hunkeler et al. (2016)) to derive the total sea ice (snow plus ice) thickness.

Snow stratigraphy was determined from up to two traditional snowpit analysis on each sampled ice floe as described in Arndt and Paul (2018).

Snow density was obtained from high-resolution snow penetrometer measurements using a SnowMicroPen (SMP, Version 4 (Schneebeli & Johnson, 1998)). The SMP was operated at a constant speed of 20 mm s^{-1} driving vertically through the snowpack while measuring the penetration force. In order to characterize the significant spatial variability, the SMP was used along 5–64 m long transect lines with a horizontal spacing of 0.5–2 m. In total, 333 profiles from the northwestern Weddell Sea and 439 profiles from the southeastern Weddell Sea are available for the subsequent analysis. Following the approach by King et al. (2020), all penetration force measurements were converted into snow density. As the maximum force was set to 41 N, the SMP stopped at hard layers, that is, icy layers and melt-freeze forms. In these cases, the bulk density of the entire snow profile is calculated as a weighted sum of the density derived from the SMP and the relative proportion of the melt-freeze forms at the bottom of the snowpack derived from snowpit analysis on each ice floe. For the melt-freeze forms, a density of 422 kg m^{-3} is assumed (Sturm et al., 1997).

2.2. Autonomous Ice-Tethered Platforms

In order to put the results of the ice station work into a broader temporal and spatial context, snow accumulation rates from snow buoys are added. Snow Buoys are autonomous measuring systems that are deployed on the sea
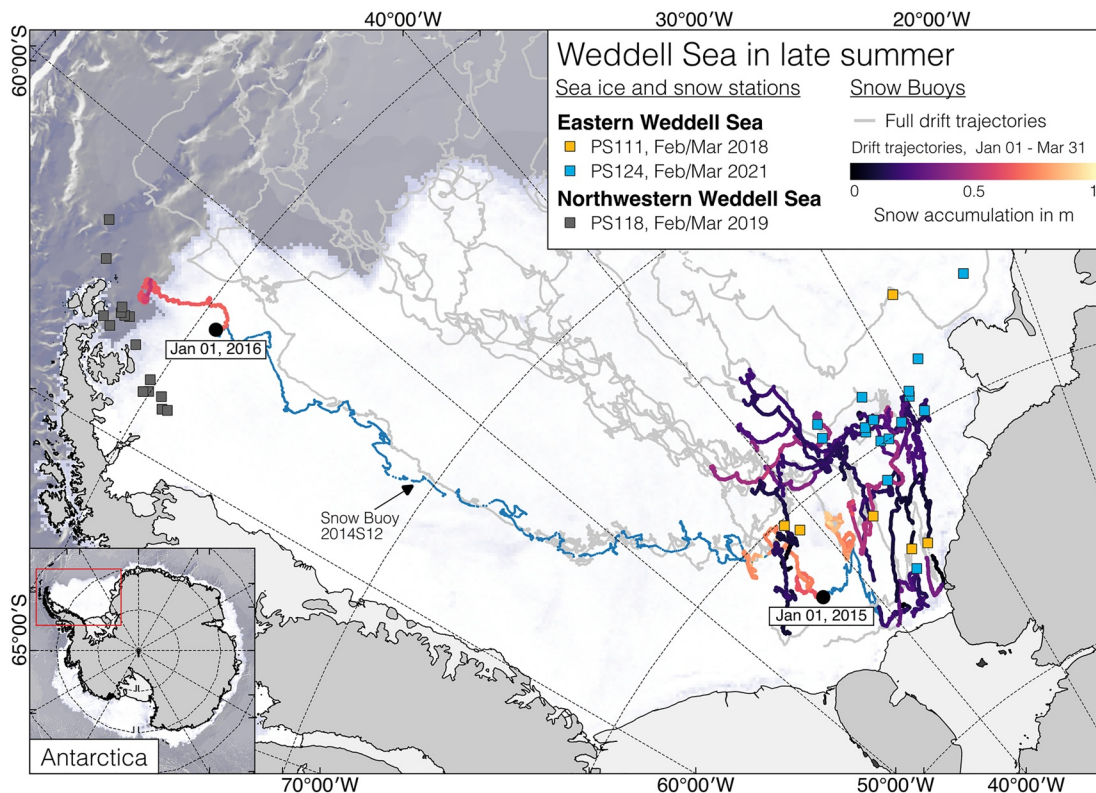
Figure 1. Overview map of all sampled ice stations of *RV Polarstern* expeditions PS111, PS118, and PS124 used in this paper. Gray lines denote the trajectories of all Snow Buoys deployed from 2013 to 2021 that included data recordings between 01 January and 31 March. The respective recorded snow accumulation within that time frame is color-coded along the trajectory. The blue line highlights the drift trajectory of Snow Buoy 2014S12 (Figure 3). Background: AMSR2 sea ice concentration from 30 March 2021 (Spreen et al., 2008).

ice and drift with it, while hourly air temperature, air pressure, and snow accumulation under four ultra sonic sensors are measured (Nicolaus et al., 2021). To put the actual data of the Snow Buoys in close context with ice station work described above, all Snow Buoys recording data in the study area of the northwestern (60–68°S, 53 to 50°W) or southeastern (70–80°S, 20 to 50°W) Weddell Sea in late summer, that is, between 01 January and 31 March, are considered (Figure 1). The respective snow accumulations of the individual Snow Buoys are given as a daily average of all four sensors.

2.3. One-Dimensional Thermodynamic Sea Ice Model

A simple one-dimensional thermodynamic ice growth model based on the number of freezing degree days (Thorndike, 1992), as used in Arndt et al. (2021), is used to estimate the potential sea ice thickness evolution along the trajectories of the Snow Buoys. The model was forced by surface temperature and heat fluxes from ERA5 reanalysis data (Copernicus Climate Change Service, 2017), daily snow accumulation from the respective Snow Buoys (see Section 2.2), and a constant oceanic heat flux of 3 Wm^{-2} (Robertson et al., 1995). For more details of the model, see Thorndike (1992) or Arndt et al. (2021). Model runs for the individual Snow Buoy trajectories are initialized with the measured sea ice thickness at the time the buoys were deployed, respectively. ERA5 reanalysis data were extracted for the nearest-neighbor grid points of the daily buoy positions. Based on this model, both thermodynamic growth at the bottom of the ice and potential ice growth at the top of the ice due to snow ice formation were calculated. For the latter, a simplified assumption is made that a calculated negative freeboard leads to a potential flooding of the snow/ice interface, which is converted into snow ice in the same time step. This assumption can be made considering that flooding occurs primarily in winter, when even with high snow accumulations, temperatures at the snow/ice interface are well below the freezing point (Arndt & Paul, 2018). In addition, this simplified ice growth model does not account for seasonalities in snow properties
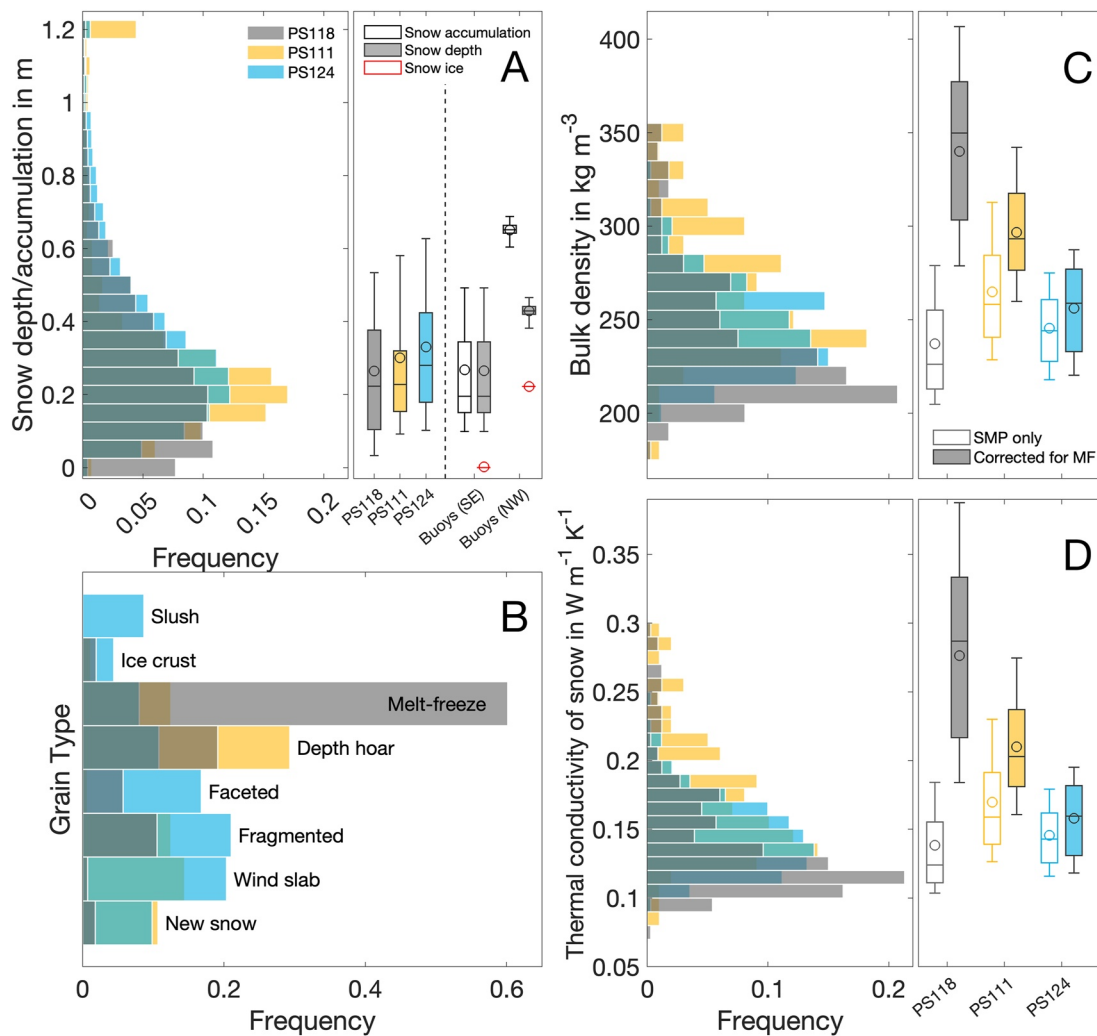
Figure 2. Relative frequency distribution function and boxplot compilations of measured and retrieved snow properties during expedition PS118 (gray), PS111 (yellow), and PS124 (blue) (a) Snow depth measured with MagnaProbe compared with the mean snow accumulation (white-filled boxes), calculated snow depth (gray-filled boxes) and calculated snow ice thickness (red circles) from Snow Buoy measurements between 01 January and 31 March (see Figure 1), separated for the southeastern and northwestern Weddell Sea (b) Grain type from snow pit measurements. (c) Bulk density and (d) thermal conductivity of snow based on vertical profiles of SnowMicroPen measurements only given in the relative distribution function and white-filled boxplots. Color-filled boxplots denote the corrected bulk density and thermal conductivity of snow based on the fraction of melt-freeze forms from the respective ice stations (see plot B). In the boxplots, boxes span over the first and third quartiles. The whiskers display the 10 and 90 percentiles. The circles indicate mean values; the solid lines indicate median values.

or ocean heat fluxes, which are, however, discussed qualitatively at the respective parts of the paper, since the accurate quantification of these processes is beyond the scope of this study.

3. Results and Discussion

3.1. Sea Ice and Snow Conditions in Late Summer

The snow regimes in the southeastern and northwestern Weddell Sea are fairly different. Installed Snow Buoys on the pack ice in the southeastern Weddell Sea recorded a mean snow height, corresponding to snow accumulation by that time, of 0.27 ± 0.20 m for the period between 01 January and 31 March, whereas the mean snow height was 0.65 ± 0.05 m in the northwest in the same time period (Figure 2a). This is attributed to the fact that the northwestern Weddell Sea contains a significant amount of perennial sea ice, while the southeastern Weddell Sea is dominated by first year ice. However, the mean snow depth measured by the Magna Probe in the northwestern Weddell Sea in February/March 2019 was 0.26 ± 0.21 m (Figure 2a), corresponding to less than half of the snow
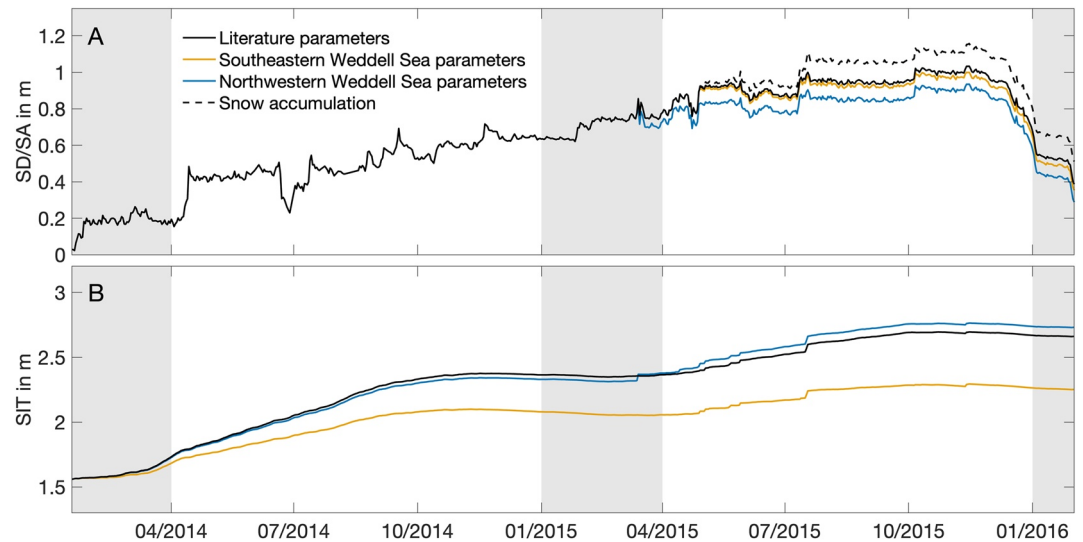
Figure 3. Time series of snow depth/accumulation (SD/SA) and sea ice thickness (SIT) along the drift trajectory of Snow Buoys 2014S12 (blue line in Figure 1) retrieved using the thermodynamic ice growth model (see Section 2.3) based on literature values (black lines) and new parameters obtained in this paper for the southeastern (yellow lines) and northwestern Weddell Sea (blue lines). Gray shaded areas mark the focus period of this study, from 01 January to 30 March. The dashed line in subplot A denotes the snow accumulation measured by the Snow Buoy.

accumulation recorded by the Snow Buoys. This contrast between snow accumulation and actual measured snow depth in the northwestern Weddell Sea in late summer is due to intense snow ice formation during the previous winter, as well as enhanced internal summer melt and refreezing in the higher latitudes leading to the formation of superimposed ice (Arndt et al., 2021). The exact quantification of the amount of snow ice for all buoys used in this study is presented in Section 3.4. In contrast, the mean measured snow depth was 0.32 ± 0.23 m for all measurements in the southeastern Weddell Sea in February/March 2018 and 2021 (Figure 2a), which is similar to the snow accumulation recorded by the Snow Buoys in late March, indicating the absence of superimposed ice and snow ice. However, for both regions, uncertainties in snow accumulation from point measurements obtained from Snow Buoys versus snow thickness measurements on floe-scale aquired during ice stations must also be considered, as well as the overall large heterogenicity of snow accumulation on sea ice.

3.2. Spatial Variability of Bulk Density

To determine the bulk density of the Antarctic snowpack, it is reasonable to divide the snow into two layers: the upper part that has undergone dry snow metamorphism and the lower one that has been subject to wet snow metamorphism, that is, has formed melt-freeze clusters (Arndt et al., 2021). For the upper part the density can be acquired with the SMP (Section 2.1), resulting in a bulk density of 250 kg m^{-3} for the southeastern Weddell Sea, and 237 kg m^{-3} for the northwestern Weddell Sea (Figure 2b). The lower density values in the northwestern Weddell Sea are due to the less compact nature of the snowpack here, as it has presumably only fallen since the onset of the snowmelt season. The part of the snowpack that has fallen on the sea ice before that has either been turned into snow ice after flooding of the snow/ice interface in winter or has internally melted during the melt season and formed into superimposed ice or the preliminary stage, that is, melt-freeze clusters. This is supported by the fact that in the northwestern Weddell Sea, the snow column consists of 60% melt freeze clusters (Figure 2c). In contrast, in the eastern Weddell Sea, the mean fraction of melt freeze clusters is only 10%. This lower part of the snowpack corresponds to the part where the SMP cannot penetrate into and also manual volumetric snow density measurements become very inaccurate. Thus, the bulk density of the total snowpack is calculated as a weighted sum based on the fraction of melt-freeze clusters in the lower snowpack with the literature-based density of 422 kg m^{-3} (Sturm et al., 1997) and the density derived from the SMP for the upper dry snowpack. Performing this calculation for each individual sampled ice floe yields a total bulk density of 264 kg m^{-3} for the southeastern Weddell Sea (Figure 2b), which is only slightly higher than the bulk density determined with the SMP due to the low fraction of melt-freeze clusters. In contrast, in the northwestern Weddell

Sea, the mean total bulk density is 340 kg m^{-3} considering the dominant high melt-freeze cluster fraction, and thus 43% higher compared to neglecting it. These results underline the importance of distinguishing between the eastern and western Weddell Sea, that is, rather seasonal and perennial sea ice, with respect to snow properties and in particular to snow density. However, such a distinction is not applied in current studies that parameterize snow density. Instead, commonly spatially and seasonally uniform density values between 300 and 320 kg m^{-3} are assumed (e.g., Fons & Kurtz, 2019; Kern et al., 2016). While Kurtz and Markus (2012), at least distinguish between different seasons, they assume 350 and 340 kg m^{-3} for summer and autumn, respectively, on pan-Antarctic-scale.

Even though the assumed density values are consistent with the measurements in the northwestern Weddell Sea, a significant discrepancy from what was measured in the eastern Weddell Sea is evident. This uncertainty propagates both to the calculation of the thermal conductivity of the sea ice and the resulting thermodynamic ice growth, as well as to the sea ice thickness products retrieved from satellite remote sensing, for the southeastern Weddell Sea respectively, as shown in the following subsections.

3.3. Sensitivity of Sea Ice Parameters to Thermal Conductivity of Snow

The thermal conductivity (k_s) of snow is a function of its snow density (ρ) and can be calculated, for example, according to Calonne et al. (2011) as follows:

$$k_s = 2.5 \cdot 10^{-6} \cdot \rho^2 - 1.23 \cdot 10^{-4} \cdot \rho + 0.024 \tag{1}$$

Even though the results represent the lower computational limit (Fourteau et al., 2022), recent snow model studies use similar assumptions (Wever et al., 2021), providing robustness to the presented sensitivities. Applying Equation 1 to the upper snowpack only, yields fairly similar mean thermal conductivity values of 0.15 and 0.14 W m^{-1} K^{-1} in the southeastern and northwestern Weddell Sea, respectively. This changes significantly when the entire snow column is considered, including the melt-freeze clusters, to 0.17 and 0.28 W m^{-1} K^{-1}, respectively, for the southeastern and northwestern Weddell Sea (Figure 2d). This difference between the two sea ice regimes arises once again from the very compact lower melt-freeze layers in the northwestern Weddell Sea, which are absent in the seasonal regime in the southeastern Weddell Sea. It is also striking that the thermal conductivity of 0.17 W m^{-1} K^{-1} in the southeastern Weddell Sea is almost half the value of 0.31 W m^{-1} K^{-1} typically assumed in thermodynamic sea ice models, such as those by Hibler (1979) and Maykut (1986), which hold to today as shown, for example, in Collins et al. (2004) and Krinner et al. (2018).

A lower thermal conductivity is directly linked to a decrease of the vertical conduction of heat through the snow and ice column and thus to a weakened thermodynamic ice growth. To quantify that effect in the eastern Weddell Sea, the ice growth was calculated along the Snow Buoy trajectories by means of a thermodynamic sea ice model (see Chapter 2.3) using the commonly used ($k_s = 0.31$ Wm^{-1}K^{-1}) and calculated ($k_s = 0.17$ Wm^{-1}K^{-1}) thermal conductivity values for the snow cover (Figure 3). Thus, until the end of March, that is, the end of summer, calculated ice thicknesses are on average 3 cm too high when using the standard values in comparison to the calculated value of thermal conductivity for the southeastern Weddell Sea. However, this difference becomes much more significant over the following winter and thus ice-growing season: until the end of November, that is, the end of spring, an overestimation of 18 cm (9%) is shown in the ice thickness calculation with the doubled thermal conductivity (Figure 3b). In a next step, the snow layer could be implemented not as a homogenous single but as a seasonal and heterogenic multilayered layer by using an appropriate snow model. Since Equation 1 is non-linear, low density snow layers would become even more important as they further reduce both the bulk thermal conductivity and ice growth. Adding snow seasonality would allow for compaction of the snow layer and thus increased thermal conductivity in winter.

A similar observation was made for the East Antarctic sea ice sector, where a mean thermal conductivity of 0.16 Wm^{-1}K^{-1} was determined from field measurements (Massom et al., 1998). In the model used in a study based on that (Fichefet et al., 2000), this led to a decrease in the ice thickness growth of 10 cm or 10%, compared to the standard thermal conductivity value, which is twice as high. Since sea ice in East Antarctica is also primarily seasonal, it highlights the need to distinguish between seasonal and perennial sea ice in snow parameterizations, not only in the Weddell Sea but on a pan-Antarctic scale, to provide a more accurate estimate of global ice growth rates.

3.4. Sensitivity of Sea Ice Parameters to Snow-to-Ice Conversion

The regional-adjusted parameters for snow density and thermal conductivity affect not only the calculation of heat fluxes between snow and sea ice and the resulting thermodynamic ice growth, but also the estimation of the amount of snow ice formed due to flooding and refreezing processes. To differentiate therefore in a next step between snow and potential snow ice within the accumulated snowpack retrieved from the Snow Buoys, the one-dimensional thermodynamic sea ice model (see Section 2.3) is applied along the drifting trajectory of the buoys, respectively. Forcing the model with the initial sea ice thickness at the time of the deployment of buoys, daily snow accumulation retrieved from the Snow Buoys, and surface temperature and heat fluxes from ERA5 reanalysis data allows to calculate both thermodynamic sea ice growth at the bottom and snow-to-ice conversion rates at the snow/ice interface. For this purpose, both regional-adjusted parameters for snow density and thermal conductivities as well as previously used literature values are used to estimate regional differences and their uncertainties. Figures 3a and 3b show the data of snow accumulation and calculated snow depth along the drift trajectory of the Snow Buoy 2014S12. The buoy was deployed in the southeastern Weddell Sea in January 2014, where it remained for one year. During this period, the calculations show no snow ice formation, that is, the snow accumulation is equal to the snow depth (Figure 3a). The offset between the calculated ice thickness growth based on the literature values to the parameterization for the southeastern Weddell Sea is therefore only caused in the different thermal conductivities applied (Figure 3b, and see Chapter 3.3). By the beginning of its second winter, the buoy drifts into the northwestern Weddell Sea. In addition, the load of the increasing snow accumulation causes the snow at the snow-ice interface to be potentially transformed into snow ice. This process remains dominant until the northerly position of the buoy as well as the onset of spring initiate surface snow melt. Based on the one-dimensional thermodynamic sea ice model initialized with the regional-adapted values, 0.22 m of potential formation of snow ice was calculated for the trajectories in the northwestern Weddell Sea, while it is only 0.12 m when using the literature values (Figure 3a). This difference is mainly due to the higher density in the northwestern Weddell Sea compared to the literature values causing a heavier snowpack and therefore more potential snow ice formation. There is high confidence in this result, given that Arndt et al. (2021) reported a similar snow ice amount on perennial sea ice in the northwestern Weddell Sea of 0.22 ± 0.22 m, while Eicken et al. (1994) discusses a snow ice proportion of 5% in the same region. Therefore, the snow accumulation of 0.65 ± 0.05 m measured by the Snow Buoys was corrected for the calculated amount of snow ice, resulting in a mean snow depth of 0.43 ± 0.23 m (HISTO A). These values are still significantly higher than the manually measured snow depth of 0.26 ± 0.21 m for the northwestern Weddell Sea (Figure 2a). The difference is caused by the fact that the simple thermodynamical sea ice model does not take the formation of superimposed ice into account which is estimated with 0.11 ± 0.11 m in previous studies (Arndt et al., 2021) and seasonal snow metamorphosm processes were not included. In addition, for simplicity, a unified ocean heat flux has been assumed for the whole Weddell Sea. However, in the deeper water regions of the Weddell Sea off the shelf, ocean heat fluxes are higher, which would lead to thinner sea ice and thus a higher probability of flooding and subsequent potential snow ice formation. Also, the unified ocean heat flux might not fully capture basal melt in summer, amplifying the effects of the sensitivity of snow-to-ice conversion.

Based on the implemented thermodynamic sea ice growth model, the sensitivity of the sea ice thickness to the snow-to-ice conversion process is determined. However, the higher amount of potentially formed snow ice in the northwestern Weddell Sea with the new parameterization for the region has also consequences for the thermodynamic ice thickness growth. As the snow ice formed has a higher thermal conductivity than the previously assumed snow layer, the total heat flux through the snow and ice column increases. This is reflected in an additional thermodynamic ice growth of 7 cm.

In contrast, for satellite-based retrievals of the Antarctic sea ice thickness, the major uncertainty does not relate to the snow density, but the lack of knowledge on snow depth and its complex diurnal and seasonal stratigraphy, causing substantial uncertainties in large-scale satellite-derived data products.

4. Summary and Conclusions

In this work, comprehensive snow measurements obtained on sea ice in the southeastern and northwestern Weddell Sea during late summer of recent years are analyzed to gain improved insights into the regionally contrasting snow structures of the area. The results show a high fraction of melt-freeze clusters in the vertical

profile of the perennial snow column in the northwestern Weddell Sea, resulting in significantly higher snow densities than in the seasonal snowpack in the southeastern Weddell Sea. For applications in remote sensing and modeling, however, a global value is assumed, as is the case for the thermal conductivity calculated from the density. Here, results of this work show that the derived thermal conductivity of 0.17 W m^{-1} K^{-1} for the southeastern Weddell Sea is almost half of the value of 0.31 W m^{-1} K^{-1} which is typically assumed. Previous studies also determined similar values for the thermal conductivity of snow in East Antarctica, which is also dominated by seasonal sea ice, as in the southeastern Weddell Sea. As seasonal sea ice is the dominant sea ice type in the ice-covered Southern Ocean, it becomes evident that a distinction between seasonal and perennial sea ice is urgently needed for an improved snow parameterizations on a pan-Antarctic scale. Such an adjustment not only results in significantly reduced sea ice growth in winter, as shown in this paper, but may also be reflected in altered sea ice-ocean interactions in coupled models, such as the resulting reduced brine release and subsequent stabilization of ocean stratification.

While a clear sensitivity of the sea ice thickness to the thermal conductivity of snow in the southeastern Weddell Sea, and thus the seasonal ice regime, is determined, this study emphasizes the importance of snow-to-ice conversion processes in the perennial ice regime in the northwestern Weddell Sea, in contrast. Here, the analysis of the accumulated snow along a drift path through the Weddell Sea revealed that potential snow ice formation adds on average 8% to sea ice growth from above in autumn in the northwestern Weddell Sea. As the formed ice has less insulating properties compared to the previous snowpack, additional thermodynamic bottom ice growth can take place. To make the snow-to-ice conversion balance complete, one would also need to compute the amount of superimposed ice, which would require the inclusion of an additional snow model and is therefore beyond the scope of this paper.

In conclusion, the example of the Weddell Sea was used to highlight the enormous impact of unappreciated regional differences in snowpack properties on thermodynamic ice growth processes. Assuming the perennial ice will retreat in times of global warming and thus the seasonal ice cover will gain in importance, it is essential that such a distinction is taken into account in both sea ice models and satellite remote sensing applications.

Conflict of Interest

The authors declare no conflicts of interest relevant to this study.

Data Availability Statement

All ERA5 data from ECMWF are accessed and downloaded from the Copernicus Climate Change Service (last access: 11 August 2021): https://cds.climate.copernicus.eu/cdsapp%23%21/dataset/reanalysis%2Dera5%2Dsingle%2Dlevels%3Ftab%3Dform. All presented field data are archived in PANGAEA with the following references: Arndt (2022b) and Arndt and Haas (2021, 2022c) for snow depth data, Arndt (2021, 2022a), and Arndt and Hass (2022b) for snow stratigraphy, and Arndt (2022c) and Arndt and Haas (2022a, 2022b), for SnowMicroPen data. Snow accumulation measurements from Snow Buoys were obtained from https://www.meereisportal.de (grant: REKLIM-2013-04) and are stored in PANGAEA (Nicolaus et al., 2017).

References

Arndt, S. (2021). Snow stratigraphy measurements at ice stations during POLARSTERN cruise PS118. *PANGAEA*. https://doi.org/10.1594/PANGAEA.929010

Arndt, S. (2022a). Snow stratigraphy measurements at ice stations during RV POLARSTERN cruise PS111. *Alfred Wegener Institute, Helmholtz Centre for Polar and Marine Research, Bremerhaven, PANGAEA*. https://doi.org/10.1594/PANGAEA.945858

Arndt, S. (2022b). Snow thickness measurements at ice stations during RV POLARSTERN cruise PS111. *Alfred Wegener Institute, Helmholtz Centre for Polar and Marine Research, Bremerhaven, PANGAEA*. https://doi.org/10.1594/PANGAEA.946183

Arndt, S. (2022c). SnowMicroPen (SMP) force profiles collected during RV POLARSTERN cruise PS111. *Alfred Wegener Institute, Helmholtz Centre for Polar and Marine Research, Bremerhaven, PANGAEA*. https://doi.org/10.1594/PANGAEA.945787

Arndt, S., & Haas, C. (2019). Spatiotemporal variability and decadal trends of snowmelt processes on Antarctic sea ice observed by satellite scatterometers. *The Cryosphere*, *13*(7), 1943–1958. https://doi.org/10.5194/tc-13-1943-2019

Arndt, S., & Haas, C. (2021). Snow thickness measurements at ice stations during POLARSTERN cruise PS118. *PANGAEA*. https://doi.org/10.1594/PANGAEA.928966

Arndt, S., & Haas, C. (2022a). SnowMicroPen (SMP) force profiles collected during RV POLARSTERN cruise PS118. *Alfred Wegener Institute, Helmholtz Centre for Polar and Marine Research, Bremerhaven, PANGAEA*. https://doi.org/10.1594/PANGAEA.945791

Arndt, S., & Haas, C. (2022b). SnowMicroPen (SMP) force profiles collected during RV POLARSTERN cruise PS124. *Alfred Wegener Institute, Helmholtz Centre for Polar and Marine Research, Bremerhaven, PANGAEA.* https://doi.org/10.1594/PANGAEA.945875

Arndt, S., & Haas, C. (2022c). *Snow thickness measurements at ice stations during RV POLARSTERN cruise PS124. PANGAEA.* https://doi.org/10.1594/PANGAEA.946177

Arndt, S., Haas, C., Meyer, H., Peeken, I., & Krumpen, T. (2021). Recent observations of superimposed ice and snow ice on sea ice in the northwestern Weddell Sea. *The Cryosphere*, *15*(9), 4165–4178. https://doi.org/10.5194/tc-15-4165-2021

Arndt, S., & Paul, S. (2018). Variability of winter snow properties on different spatial scales in the Weddell Sea. *Journal of Geophysical Research: Oceans*, *123*(12), 8862–8876. https://doi.org/10.1029/2018JC014447

Arndt, S., Stoll, N. A., Winkelmann, R., Reese, R., & Huntemann, M. (2018). Chapter sea ice physics in: The expedition PS111 of the research POLARSTERN to the southern Weddell Sea in 2018. *Berichte zur Polar-und Meeresforschung= Reports on polar and marine research*, *718*, 30–52. https://doi.org/10.2312/BzPM_0718_2018

Arndt, S., Willmes, S., Dierking, W., & Nicolaus, M. (2016). Timing and regional patterns of snowmelt on Antarctic sea ice from passive microwave satellite observations. *Journal of Geophysical Research - Oceans*, *121*(8), 5916–5930. https://doi.org/10.1002/2015JC011504

Calonne, N., Flin, F., Morin, S., Lesaffre, B., du Roscoat, S. R., & Geindreau, C. (2011). Numerical and experimental investigations of the effective thermal conductivity of snow. *Geophysical Research Letters*, *38*(23). https://doi.org/10.1029/2011gl049234

Collins, W. D., Rasch, P. J., Boville, B. A., Hack, J. J., McCaa, J. R., Williamson, D. L., et al. (2004). Description of the NCAR community atmosphere model (CAM 3.0). *NCAR Tech. Note NCAR/TN-464+ STR*, *226*, 1326–1334.

Copernicus Climate Change Service. (2017). ERA5: Fifth generation of ECMWF atmospheric reanalyses of the global climate. Retrieved from https://cds.climate.copernicus.eu/cdsapp%23%21/home

Eicken, H., Lange, M. A., Hubberten, H. W., & Wadhams, P. (1994). Characteristics and distribution patterns of snow and meteoric ice in the Weddell Sea and their contribution to the mass balance of sea ice. *Annales Geophysicae-Atmospheres Hydrospheres and Space Sciences*, *12*(1), 80–93. https://doi.org/10.1007/s00585-994-0080-x

Fichefet, T., Tartinville, B., & Goosse, H. (2000). Sensitivity of the Antarctic sea ice to the thermal conductivity of snow. *Geophysical Research Letters*, *27*(3), 401–404. https://doi.org/10.1029/1999gl002397

Fons, S. W., & Kurtz, N. T. (2019). Retrieval of snow freeboard of Antarctic sea ice using waveform fitting of CryoSat-2 returns. *The Cryosphere*, *13*(3), 861–878. https://doi.org/10.5194/tc-13-861-2019

Fourteau, K., Hagenmuller, P., Roulle, J., & Domine, F. (2022). On the use of heated needle probes for measuring snow thermal conductivity. *Journal of Glaciology*, *68*(270), 705–719. https://doi.org/10.1017/jog.2021.127

Haas, C., Arndt, S., Peeken, I., & Allhusen, E. (2019). Chapter sea ice in: The expedition PS118 of the research vessel POLARSTERN to the Weddell Sea in 2019. *Berichte zur Polar-und Meeresforschung= Reports on polar and marine research*, *735*, 97–123. https://doi.org/10.2312/BzPM_0735_2019

Haas, C., Arndt, S., Peeken, I., Eggers, S. L., & Neudert, M. (2021). Chapter sea ice geophysics and biogeochemistry in: The expedition PS124 of the research vessel POLARSTERN to the Weddell Sea in 2021. *Berichte zur Polar-und Meeresforschung= Reports on polar and marine research*.

Hibler, W. D. (1979). A dynamic thermodynamic sea ice model. *Journal of Physical Oceanography*, *9*(4), 815–846. https://doi.org/10.1175/1520-0485(1979)009<0815:adtsim>2.0.co;2

Hunkeler, P. A., Hendricks, S., Hoppmann, M., Farquharson, C. G., Kalscheuer, T., Grab, M., et al. (2016). Improved 1D inversions for sea ice thickness and conductivity from electromagnetic induction data: Inclusion of nonlinearities caused by passive bucking. *Geophysics*, *81*(1), Wa45–Wa58. https://doi.org/10.1190/Geo2015-0130.1

Jena, B., Bajish, C. C., Turner, J., Ravichandran, M., Anilkumar, N., & Kshitija, S. (2022). Record low sea ice extent in the Weddell Sea, Antarctica in April/May 2019 driven by intense and explosive polar cyclones. *npj Climate and Atmospheric Science*, *5*(1), 19. https://doi.org/10.1038/s41612-022-00243-9

Kern, S., Ozsoy-Çiçek, B., & Worby, A. P. (2016). Antarctic Sea-ice thickness retrieval from ICESat: Inter-comparison of different approaches. *Remote Sensing*, *8*(7), 538. https://doi.org/10.3390/rs8070538

King, J., Howell, S., Brady, M., Toose, P., Derksen, C., Haas, C., & Beckers, J. (2020). Local-scale variability of snow density on Arctic sea ice. *The Cryosphere*, *14*(12), 4323–4339. https://doi.org/10.5194/tc-14-4323-2020

Krinner, G., Derksen, C., Essery, R., Flanner, M., Hagemann, S., Clark, M., et al. (2018). ESM-SnowMIP: Assessing snow models and quantifying snow-related climate feedbacks. *Geoscientific Model Development*, *11*(12), 5027–5049. https://doi.org/10.5194/gmd-11-5027-2018

Kurtz, N., & Markus, T. (2012). Satellite observations of Antarctic sea ice thickness and volume. *Journal of Geophysical Research*, *117*(C8). https://doi.org/10.1029/2012jc008141

Lee, S. K., Volkov, D. L., Lopez, H., Cheon, W. G., Gordon, A. L., Liu, Y. Y., & Wanninkhof, R. (2017). Wind-driven ocean dynamics impact on the contrasting sea-ice trends around West Antarctica. *Journal of Geophysical Research-Oceans*, *122*(5), 4413–4430. https://doi.org/10.1002/2016jc012416

Massom, R., Eicken, H., Hass, C., Jeffries, M. O., Drinkwater, M. R., Sturm, M., et al. (2001). Snow on Antarctic sea ice. *Reviews of Geophysics*, *39*(3), 413–445. https://doi.org/10.1029/2000rg000085

Massom, R., Lytle, V. I., Worby, A. P., & Allison, I. (1998). Winter snow cover variability on East Antarctic sea ice. *Journal of Geophysical Research*, *103*(C11), 24837–24855. https://doi.org/10.1029/98jc01617

Maykut, G. A. (1986). The surface heat and mass balance. In *The geophysics of sea ice* (pp. 395–463). Springer, University of Washington.

Nicolaus, M., Haas, C., & Willmes, S. (2009). Evolution of first-year and second-year snow properties on sea ice in the Weddell Sea during spring-summer transition. *Journal of Geophysical Research*, *114*, D17109. https://doi.org/10.1029/2008JD011227

Nicolaus, M., Hoppmann, M., Arndt, S., Hendricks, S., Katlein, C., König-Langlo, G., et al. (2017). Snow height and air temperature on sea ice from Snow Buoy measurements. *Alfred Wegener Institute, Helmholtz Centre for Polar and Marine Research, PANGAEA.* https://doi.org/10.1594/PANGAEA.875638

Nicolaus, M., Hoppmann, M., Arndt, S., Hendricks, S., Katlein, C., Nicolaus, A., et al. (2021). Snow depth and air temperature seasonality on sea ice derived from snow buoy measurements. *Frontiers in Marine Science*, *8*(377). https://doi.org/10.3389/fmars.2021.655446

Parkinson, C. L., & DiGirolamo, N. E. (2021). Sea ice extents continue to set new records: Arctic, Antarctic, and global results. *Remote Sensing of Environment*, *267*, 112753. https://doi.org/10.1016/j.rse.2021.112753

Robertson, R., Padman, L., & Levine, M. D. (1995). Fine structure, microstructure, and vertical mixing processes in the upper ocean in the Western Weddell Sea. *Journal of Geophysical Research*, *100*(C9), 18517–18535. https://doi.org/10.1029/95jc01742

Schneebeli, M., & Johnson, J. B. (1998). A constant-speed penetrometer for high-resolution snow stratigraphy. *Annals of Glaciology*, *26*, 107–111. https://doi.org/10.3189/1998aog26-1-107-111

Spreen, G., Kaleschke, L., & Heygster, G. (2008). Sea ice remote sensing using AMSR-E 89-GHz channels. *Journal of Geophysical Research-Oceans*, *113*(C2), C02S03. https://doi.org/10.1029/2005jc003384

Sturm, M., & Holmgren, J. (2018). An automatic snow depth probe for field validation campaigns. *Water Resources Research*, *54*(11), 9695–9701. https://doi.org/10.1029/2018wr023559

Sturm, M., Holmgren, J., Konig, M., & Morris, K. (1997). The thermal conductivity of seasonal snow. *Journal of Glaciology*, *43*(143), 26–41. https://doi.org/10.1017/s0022143000002781

Sturm, M., Morris, K., & Massom, R. (1998). The winter snow cover of the west Antarctic pack ice: Its spatial and temporal variability. *Antarctic Sea Ice: Physical Processes, Interactions and Variability Antarctic Research Series*, *74*, 1–18.

Thorndike, A. (1992). A toy model linking atmospheric thermal radiation and sea ice growth. *Journal of Geophysical Research*, *97*(C6), 9401–9410. https://doi.org/10.1029/92jc00695

Tian, L. J., Gao, Y. L., Weissling, B., & Ackley, S. F. (2020). Snow-ice contribution to the structure of sea ice in the Amundsen Sea, Antarctica. *Annals of Glaciology*, *61*(83), 369–378. https://doi.org/10.1017/aog.2020.55

Vernet, M., Geibert, W., Hoppema, M., Brown, P. J., Haas, C., Hellmer, H., et al. (2019). The Weddell gyre, Southern Ocean: Present knowledge and future challenges. *Reviews of Geophysics*, *57*(3), 623–708. https://doi.org/10.1029/2018rg000604

Wever, N., Leonard, K., Maksym, T., White, S., Proksch, M., & Lenaerts, J. T. (2021). Spatially distributed simulations of the effect of snow on mass balance and flooding of Antarctic sea ice. *Journal of Glaciology*, *67*(266), 1–19. https://doi.org/10.1017/jog.2021.54